Evolution of Drought Mitigation and Water Security through 100 Years of Reservoir Expansion in Semi-Arid Brazil.

Antônio Alves Meira Neto[1*], Pedro Medeiros[2], José Carlos de Araújo[3], Bruno Pereira[3] Murugesu Sivapalan[4,5]

[1] Department of Civil and Environmental Engineering, Colorado State University, Fort Collins, CO, USA.

[2] Federal Institute of Education, Science and Technology of Ceará, Fortaleza, Brazil

[3] Federal University of Ceará, Fortaleza, Brazil

[4] Department of Geography and Geographic Information Science, University of Illinois at Urbana-Champaign, Urbana, USA

[5] Department of Civil and Environmental Engineering, University of Illinois at Urbana-Champaign, Urbana, USA

*Corresponding author: ameira@colostate.edu

Key points

1. A hydrologic model with evolving structure was developed to capture 100 years of reservoir expansion in a large semi-arid basin.
2. Hydraulic expansion led to an increase in water security over that century.
3. Drought intensity and duration evolved differently through the system, with smaller reservoirs becoming more vulnerable over time.

ABSTRACT

Early peopling of Brazil's Northeast region (BRN) took place under an intimate relationship between humans and water scarcity, as the region, especially the state of Ceará (CE), has dealt historically with severe drought events since the 1800's, which commonly led to catastrophic impacts of mass migration and deaths of thousands of people. Throughout the last century, the so-called "Droughts Polygon" region experienced intense infrastructural development, with the expansion of a dense network of reservoirs. This resulted in the evolution of a complex hydrologic system requiring a holistic investigation in terms of its hydrologic tradeoffs. This paper presents a parsimonious hydrologic modeling approach to investigate the 100-year (1920-2020) evolution of a dense surface-water network in the 24,500 km² Upper Jaguaribe Basin, with the ultimate goal of generating insights into the coevolution of a tightly coupled human-water system. Our model is driven by both climatic and human inputs, while model structure is allowed to evolve over time to dynamically mimic evolution of population size, reservoir count and water demand. Hundred years of continuous growth in storage capacity experienced within the UJ Basin is found to reflect the transition from complete vulnerability to droughts to achievement of significantly increased levels of water security. However, drought severity had in the meantime disproportionally intensified in this period, especially in reservoirs of medium to small capacities. Our analysis results have generated valuable insights into the different roles that reservoir expansion has played in securing the stability of human settlement patterns in drought prone regions.

1. Introduction

Brazil's Northeast (BRN) region, especially its semi-arid portion, has been historically plagued by frequent droughts dating all the way back to the 1800's. The occurrence of the "Great Drought" and other similar drought events (Guerra, 1981. Neves, 2007) have been extensively reported in historical records, and are deeply entrenched in people's collective memory, becoming an integral part of the folklore and culture of the region. The history of development in the Upper Jaguaribe (UJ) Basin, which is located within the state of Ceará, is typical of how the growth of human populations have coevolved with the development of water resources in Brazil's driest region, having experienced intense growth of reservoir storage capacity through the construction of a series of dams over the last century (Malveira et al., 2012; de Araújo and Bronstert, 2016; Pereira et al., 2019; Medeiros and Sivapalan, 2020;).

The implementation of storage reservoirs has been a common approach to mitigate water scarcity in arid and semi-arid regions around the world where surface water yields of catchments are not able to meet the growing human water demand, especially in scenarios in which economical and/or political interests favor this approach over others (Cai et al., 2008; van der Zaag and Gupta, 2008; Campos, 2015; Abeywardana et al., 2018). Also referred to as a hard-path solution (Medeiros and Sivapalan, 2020), the construction of dams has been widely employed elsewhere as a strategy not only for mitigating water scarcity (Peter et al., 2014; Di Baldassarre et al., 2018), but also for flood and drought mitigation, by buffering the natural inter- and intra-annual variability in precipitation and streamflow.

It is becoming increasingly clear that, despite its positive socioeconomic impact, the construction of surface reservoirs may in the long term give rise to unintended consequences, such as increased water demand, a human tendency triggered by perceptions of increased water availability resulting from reservoir construction (Di Baldassarre et al., 2018; Habets et al., 2018; Ribeiro Neto et al., 2022; van Langen et al., 2022). Perceptions of improved water security brought about by the construction of reservoirs tend to persist in society, giving rise to unregulated and unplanned growth of both human populations and reservoir construction. An example is the development of dense reservoir networks in the Ceará region in Brazil over the last century (Malveira et al., 2012; de Araújo and Bronstert, 2016; Pereira et al., 2019; Medeiros and Sivapalan, 2020). The socio-

economic-political and hydrologic factors that may have contributed to this phenomenon are still poorly understood nor fully accounted for.

The acknowledgment and assessment of both the intended and unintended consequences of reservoir expansion, including mitigation of water scarcity and possible aggravation of drought events, is of utmost importance for understanding the long-term implications of such hard infrastructure solutions and longer-term policy decisions (Ribeiro Neto et al., 2022). Therefore, a comprehensive understanding of the nature of co-evolution of human-water system feedbacks and the hydrological and socio-political drivers that might lead to emergence of the observed phenomena (e.g., increasing dam density) are needed for clarifying the circumstances under which such phenomena might emerge. This calls for a new generation of hydrological models that accommodate human-water system co-evolution and support both assessment of the impacts as well as shed light on the socio-economic mechanisms that underpin this coevolution.

Capturing the hydrological functioning of such a large network of reservoirs poses major challenges to the modeling exercise, due to the need for specific reservoir properties and operation rules for each unit within the system, which are commonly not available. Moreover, in the global South, socio-political conditions prevailing in water scarce regions are normally associated with poor monitoring of such diffuse systems, a problem further aggravated in locations where reservoirs are built by local cooperatives and private landowners. This is certainly the case in the Ceará region in Brazil. To deal with water management in such data-scarce regions and yet achieve meaningful hydrologic representation of socio-hydrological processes, a lumped hydrologic representation of reservoir systems has often been adopted (Güntner et al., 2004). Lumped-systems hydrological modeling approaches can also take advantage of readily available remote-sensing data to quantify and temporally assess the density of reservoir units in regions where on-ground information is not available (Heine et al., 2014; Zhang et al., 2016; Pereira et al., 2019).

Our hydrologic data record spans 100 years (1920-2020) of measured precipitation, runoff, and meteorological variables in the Upper Jaguaribe, a 24,500 km^2 semi-arid basin that has experienced a 100-fold increase in artificially built storage capacity throughout the last century. We couple a lumped, conceptual hydrologic model to a lumped reservoir system model and use historical data on reservoir construction, paired with demographic data, to simulate the system's reservoir

capacity and population growth from its initially pristine state to its current highly altered condition, i.e., through an evolving model structure. Simulations with this dynamic model are then used to track advances in water security and the mitigation of water scarcity brought about by the build-up of reservoir capacity, including how well reservoir storage may have either helped to mitigate against or further exacerbate the sequence of major droughts that have periodically hit the region over the century.

2. Study Area

The Upper Jaguaribe (UJ) basin (24500 km^2) is located within the state of Ceará, in the Northeast region of Brazil (**Figure 1a**). It is characterized by a semi-arid climate, with mean annual precipitation of 700 $mm.y^{-1}$ and mean annual potential evaporation of 2100 $mm.y^{-1}$. Rainfall is concentrated in the summer months (Jan-Mar, **Figure 1b**) with marked inter-annual variability (coefficient of variation of 30%), as seen in **Figure 1c**. Runoff coefficients typically vary between 5 and 10% in the region and can at times be as low as 1% (de Figueiredo et al., 2016), while rivers are mainly ephemeral (Malveira et al., 2012; Mamede et al., 2018). Crystalline bedrock and shallow soils characterize basin's substrate, while the vegetation is typical of the Brazilian Caatinga biome (mainly xerophytic woodland). The economy of the rural areas in the basin revolves around extensive cattle farming and subsistence agriculture, consisting mainly of rainfed beans and corn cultures (van Oel et al., 2008). The average Human Development Index (HDI) in the 27 municipalities that make up the UJ basin is 0.605 and the average GDP per capita is approximately US$ 2050.00 per year.

Dam construction within the Jaguaribe basin commenced in the 1900's, intensifying from the 1960's up to the 1990's through the construction of numerous large and small reservoirs by both state-led initiatives and private owners. For much of the last century, reservoir construction was adopted by the government and the private sector as a major strategy to respond to increasing drought risk caused by rapid population growth. Reservoir construction rate has been slowly falling in the region in recent times, as alternative (soft path) solutions to balance water supply and demand have been attempted. A more detailed account of reservoir construction strategy within Jaguaribe basin, which encompasses the UJ basin, can be found in Medeiros and Sivapalan (2020).

We used the Global Surface Water Explore (https://global-surface-water.appspot.com/) (Pekel et al., 2016) product for estimating the current total reservoir count and considered only reservoirs with area greater than 1 ha in this count. This process led to a total of 3500 reservoirs that exist currently within the UJ basin, with storage capacities ranging from less than 1.0 x 10^5 m³ to larger than 1.94 x 10^9 m³.

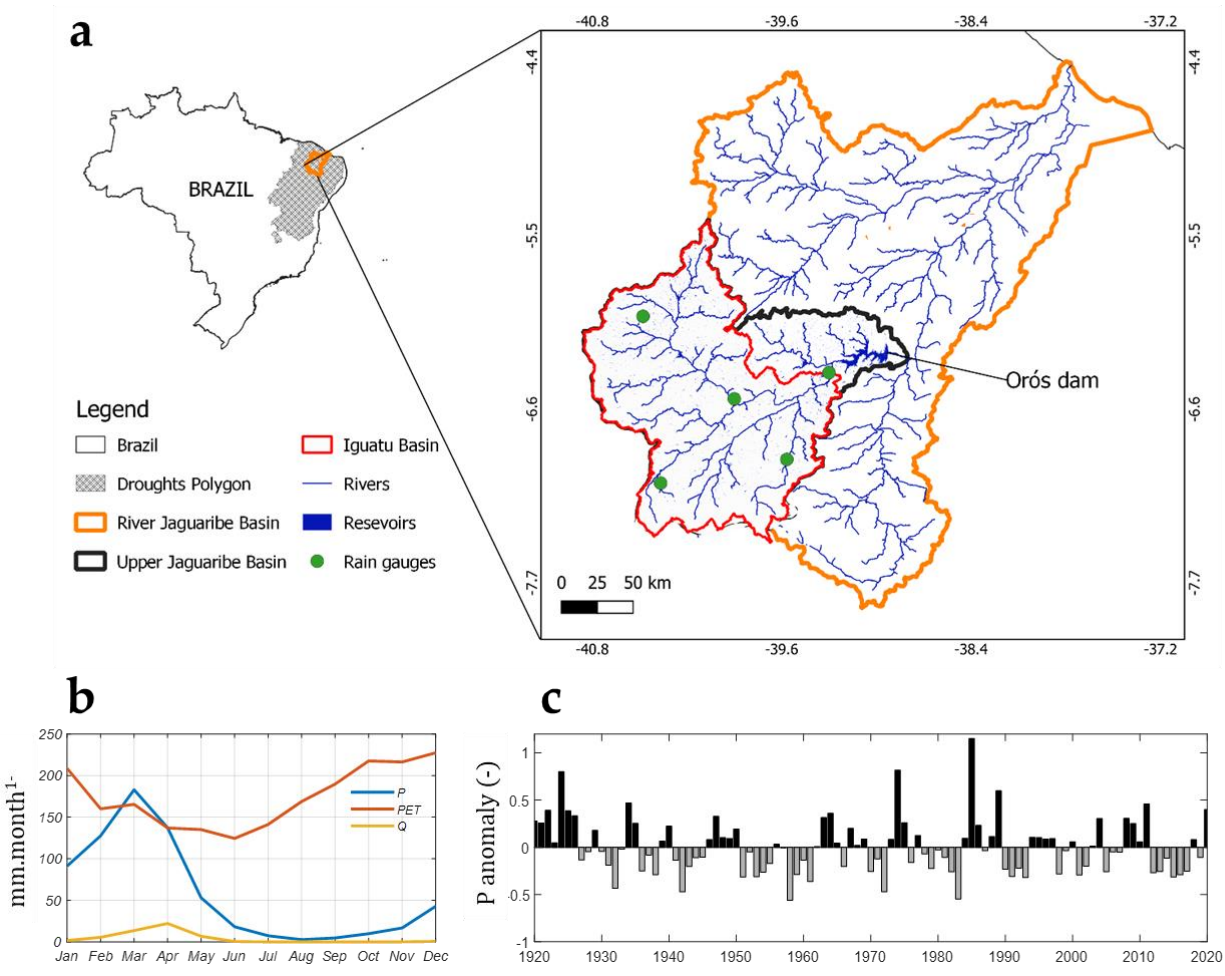

Figure 1. Study area: a - Location, with details of the Iguatu contributing area, as well as the Upper Jaguaribe basin. b - Mean-monthly values of precipitation (P), potential evaporation (PET) and streamflow (Q) for the Iguatu station. c - Interannual precipitation variability, shown as % deviation of mean value throughout the study period.

3. Hydrologic Modeling

Our modeling approach is divided into two parts. *Part 1* refers to the modeling of the Iguatu (IG) sub-basin, which was used to calibrate the hydrologic model HYMOD for the 1920-1940 decades, hereafter named as the undisturbed period due to minimal infrastructure construction during that period. The IG basin accounts for 80% of the Upper Jaguaribe area and was selected due to the availability of streamflow measurements. This calibrated model is assumed to represent runoff production during the basin's more pristine conditions. Model performance was then tested for the period between 1950 and 2020, which we define as the disturbed period. Both undisturbed and disturbed periods are broad classifications to separate the decades with reduced influence of reservoirs from the decades when reservoir construction experienced a boom. This classification was done based on local knowledge and applies to both IG and UJ basins. After model calibration and validation, we implemented the reservoir system model (RSM) as an additional routing step to the HYMOD-generated streamflow. The combined HYMOD-RSM approach was developed to incorporate the effects of the expansion of the reservoir network over multiple decades. We validated this approach by comparing the newly generated streamflow values against observed ones at the IG station for the undisturbed period.

In *Part 2*, we applied the previously calibrated HYMOD-RSM model to the UJ basin and used the observed values of water storage at the Orós reservoir (the largest reservoir, which is located at the basin's outlet) for validation. Following that, we perform diagnostic analyses with the model to further investigate the effects of the reservoir system's growth on hydrologic fluxes and states, while also investigating the role of the systems dynamic in shaping water fluxes, storage and meeting water demand in the region.

3.1. The modified HYMOD

We implemented a modified version of the HYMOD hydrologic model. HYMOD is a spatially lumped, conceptual rainfall-runoff model consisting of six parameters and has been used in several studies (for instance, Boyle et al., 2000; Wang et al., 2009; Quan et al., 2014; Roy et al., 2017). A brief explanation of the model's functioning is presented here, along with the changes

implemented as part of this study. A more thorough discussion on the model structure and parameters can be found in the references listed above.

The model uses daily inputs of precipitation (P) and potential evapotranspiration (PET) to generate estimates of actual evapotranspiration (AE) and streamflow (Q). It assumes a spatially distributed soil moisture storage (S) according to the following relationship:

$$S(t) = S_{max}\left(1 - \left(1 - \frac{H(t)}{H_{max}}\right)^{1+b}\right) \quad (1)$$

in which S_{max} represents the maximum storage capacity (mm), H is the storage height, H_{max} is the maximum storage height, and b is the distribution function shape parameter relating S_{max} to H_{max}:

$$S_{max} = \frac{H_{max}}{1+b} \quad (2)$$

At each time step, an initial estimate of S is computed (S_{beg} from the initial height (H_{beg}), following Equation 1. After that, with the addition of precipitation, an initial estimate of overland flow (OV) is computed as:

$$OV = \left(0, P + H_{beg} - H_{max}\right) \quad (3)$$

The infiltration (I) is then obtained as:

$$I = P - OV \quad (4)$$

Following that, an intermediate storage height (H_{int}) is calculated as:

$$H_{int} = I + H_{beg} \quad (5)$$

which will lead to an intermediate storage (S_{int}) calculated using Equation 1. Finally, the interflow (IF), is computed as:

$$IF = S_{beg} + I - S_{int} \quad (6)$$

PET is then used to compute the actual evapotranspiration, which will lead to the updated storage at the end of the time step, S_{end}:

$$ET = (PET, S_{int}) \quad (7)$$

$$S_{end} = S_{int} - ET \quad (8)$$

The sum of IF and OV leads to the total runoff (TR = IF + OV), which is separated into a fast (Q_{fast}) and slow component (Q_{slow}), using a split parameter, α:

$$Q_{fast} = \alpha * TR \quad (9)$$

$$Q_{slow} = TR - Q_{fast} \quad (10)$$

Q_{fast} is then routed through a series of "n" linear reservoirs in series, each with the same release constant (K_q), i.e., a Nash cascade routing scheme, while slow flow is routed through a single linear reservoir with a K_s release constant. The slow flow linear reservoir is modified with the addition of a threshold parameter γ that defines the minimum amount of storage in the slow flow reservoir so that release can occur. This modification was attempted after the observation of poor model performance during dry months, when no flow occurred, which was not adequately simulated through the model. A schematic showing the HYMOD components and parameters is shown in **Figure 2a**.

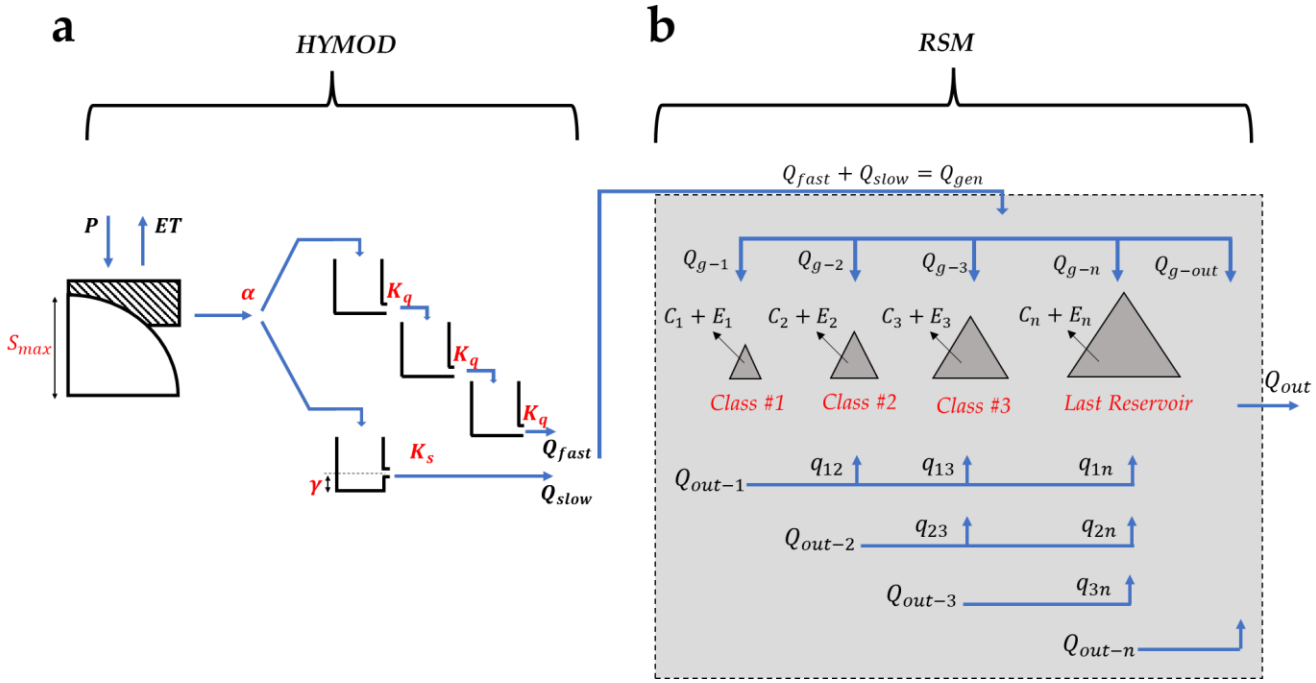

Figure 2. The modelling approach used in this study. a – Streamflow production using HYMOD. b – Schematic representation of the reservoir system model (RSM), showing the aggregation of reservoirs into classes, along with the runoff routing through the system as well as the imposed demands and evaporation fluxes.

3.2. HYMOD Calibration and Validation

We calibrated the HYMOD model over the 1920-1950 period, during which we assume human influence to be minimal and the impact of reservoirs can be considered negligible. As mentioned previously, this approach ensures that the calibrated model can be considered as representative of a non-disturbed system, and that the runoff is generated under natural conditions. Model calibration was conducted to reproduce the streamflow measured at the Iguatu station (Figure 1). We used a semi-automated procedure, consisting of first fitting the model using the Shuffled Complex Evolution (SCE-UA, Duan et al., 1992), with the Nash-Sutcliffe Efficiency (NSE) metric as the objective function. For that, we used monthly values of observed and simulated streamflow (in mm per month). After this initial procedure, we've manually adjusted the model parameters to obtain unbiased (assessed through slope of the linear regression between observed and simulated monthly values) estimates of streamflow production. Once calibrated, we compared simulated values of streamflow for the disturbed period (1950-2020) through both NSE and Bias estimates, using both HYMOD only, as well as the HYMOD-RSM approach, which is be described below.

3.3. Reservoir System Model (RSM)

The approach adopted to simulate the reservoir system at the UJ basin, hereafter named RSM, is based on the model proposed by Güntner et al. (2004). RSM is a lumped model where the reservoir system is separated into different classes according to the reservoirs' storage capacities. For each reservoir class, the water balance is computed considering a single representative reservoir (RR) in which local fluxes (evaporation and withdrawals) along with state variables (local volume and height) are estimated. The RR has a storage capacity equal to the average capacity observed for that class, as well as depth-volume-area relationships representing average conditions for that class. The model considers a cascade-type routing of the runoff, as well as the propagation of the unmet demands between different capacity classes. The RSM was developed and tested for the local conditions of the Droughts Polygon, including the UJ basin, and was able to satisfactorily simulate volumes of both small and large reservoirs within that region (Güntner et al., 2004, Malveira et al., 2012, Bronstert et al., 2014, Mamede et al., 2018). The following section describes the RSM formulations in detail.

3.3.1. Reservoir classes and evolution of the reservoir network

The RSM assumes the division of the reservoirs into a given number of classes. In this study, we adopted a total of six classes, as shown in **Table 1**. This scheme was followed for simulations of both the IG as well as the UJ basins under disturbed conditions (1950-2020). While for classes 1 through 5 an actual aggregation of different reservoirs into classes is performed, class 6 is represented by the largest reservoir within the basin, with capacity equal to V_{RL} (hm^3). The adopted approach enables one to parsimoniously simulate networks with thousands of reservoirs (see **Table 1**), combining reasonable efforts with low data entry, which is particularly important in regions where information on small dams is scarce, such as in the study area (Pereira et al., 2019, Zhang et al., 2016). The class ranges were defined based on the distribution of reservoirs and respective storage capacities.

Table 1. Subdivision of reservoir system into classes, along with their hydraulic properties for both Iguatu (IG) and Upper Jaguaribe (UJ) basins used in this study. Star (*) symbol denotes hydraulic properties of a single reservoir (class 6).

Class Nr.	Volume Range (hm^3)		Res. Count		Total Volume (hm^3)		Avg Volume (hm^3)		Avg α		Avg K	
	Min	Max	IG	UJ	IG	UJ	IG	UJ	IG	UJ	IG	UJ
1	0.0	0.1	2127	2969	44	61	0.0	0.0	2.7	2.7	1120	1120
2	0.1	0.5	296	373	61	77	0.2	0.2	2.9	2.8	1432	1844
3	0.5	1.0	49	61	34	42	0.7	0.7	3.0	3.0	1167	1699
4	1.0	20.0	50	64	159	226	3.2	3.5	3.1	3.1	1468	3900
5	20.0	V_{RL}	8	10	320	742	40.0	74.2	3.4	3.7	2408	2702
6	V_{RL}		1	1	197	1940	197.0*	1940*	3.0*	4.4*	10902*	210*

We represent the evolution of the reservoir network over time by tracking the increase in the total number of strategic reservoirs, i.e., those used to supply cities and large demand centers, which are monitored by the local water management company, for which construction dates and design characteristics are known. We used this subset to generate a relationship between storage capacity (in % of the capacity observed in the present) versus year for both IG and UJ basins. A total of 20 reservoir records were used for the estimation of capacity curve for the IG basin, whereas a total of 25 reservoir records were used for the UJ basin. It is worth noting that reservoirs contained in the subset used in the estimation of the system evolution belonged to classes 4 and 5 only, and that no data was available on the construction of lower-class reservoirs. The hypothesis that the increase rate of the system storage capacity approaches that of the strategic reservoirs can be supported by the fact that, the spontaneous construction of small dams by the rural population was encouraged by the success of strategic dams on supplying water, therefore it is expected that it followed the public policy of reservoir construction. Furthermore, the strategic reservoirs (mostly classes 5 and 6) account for over 85% of the system capacity in the UJ basin, although in much lower number (**Table 1**). The list of reservoirs, including names, storage capacities and construction dates are shown in the supplementary material (**Table S1**). Finally, the number of reservoirs per class in each year was then computed by multiplying the system's percent capacity in a given year, estimated as described above, by the total (current) number of reservoirs per class.

3.3.2. Distribution of the generated runoff

The runoff produced by HYMOD during a given time step (Q_g, in m³) is distributed into fractions contributing to each reservoir class (Q_{g-n} , in m³), along with the runoff that is directly routed to the catchment outlet (Q_{g_out}, in m³/day)

$$Q_g(t) = \left(\sum_{n=1}^{N} Q_{g-n}(t)\right) + Q_{g-out}(t) \quad (11)$$

Both Q_{g-n} and Q_{g-out} are estimated based on time-varying fractions:

$$Q_{g-n}(t) = f_n(t) \cdot Q_g(t) \quad (12)$$

$$Q_{g-out}(t) = f_{out}(t) \cdot Q_g(t) \quad (13)$$

where $f_n$represents the fraction of Q_g contributing to the nth class at a given time, and f_{out} the fraction of Q_g not contributing to any reservoir class, and thus directly routed to the catchment's outlet. The f_n values varied according to the total capacity in each class at a given moment in time. To estimate f_n we first assumed the following empirical relationship between storage capacity and incoming mean annual runoff:

$$C_n(t) = 2 \cdot \bar{Q}_n(t) \quad (14)$$

where C_n represent the storage capacity of class n (m^3), and $\overline{Q}_n$ the mean annual incoming runoff of class n (m^3). Although simplistic, the relationship indicated in Equation 14 has been shown to hold for several reservoirs within the study region (Campos, 2015; de Araújo and Bronstert, 2016) and represents a rule-of-thumb approach for reservoir construction used by the local population. Indeed, Aguiar (1978) sized seven strategic reservoirs in the Droughts Polygon during the 20th Century, in which the ratio between accumulation capacity and annual inflow volume varies from 1.71 (Piranhas reservoir) to 2.48 (Cedro reservoir), the average value being 2.07. Interestingly, the same relationship is approximately held when taking the whole reservoir system within the AJ basin, thus serving as a large-scale validation of the rationale implemented at the local scale. Given

the known values of C_n, Equation 14 is used to produce estimates $\overline{Q}_n$. Following that, we defined f_n as the ratio between $\overline{Q}_n$ and the mean annual runoff observed for the whole basin ($\overline{Q}_B$):

$$f_n(t) = \frac{\bar{Q}_n(t)}{\bar{Q}_B} = \frac{C_n(t)}{2 \cdot \bar{Q}_B} \quad (15)$$

The fraction of the generated runoff contributing directly to the catchments' outlet ($f_{out}(t)$) is then obtained as:

$$f_{out}(t) = 1 - \sum_{n=1}^{N} f_n(t) \quad (16)$$

3.3.3. Runoff routing and water balance at reservoir classes

The runoff produced at each time-step is routed through the reservoir system assuming a cascade-type scheme. For each reservoir class, the incoming runoff (Q_{-n}, in m^3) is composed of Q_{g-n} and the contribution from the outflow of the preceding (lower classes) reservoirs:

$$Q_{in-n}(t) = Q_{g-n}(t) + \sum_{1}^{n-1} \frac{Q_{out-\mathrm{x}}(t)}{N - \mathrm{x}} \quad (17)$$

where Q_{out-x} is the outflow generated by a lower (x < n) reservoir class, where x is a dummy variable. The sum term in Equation 17 means that the outflow from each reservoir class is uniformly distributed among the higher-class reservoirs. For example, the outflow from class 2 (Q_{out-2}) will be distributed in 4 equal parts ($\frac{Q_{out-2}}{4}$) among classes 3, 4, 5 and 6. For each reservoir class, the water balance equation is then solved for the representative reservoir:

$$V_n(t) = V_n(t-1) + \frac{Q_{in-n}(t)}{R_c(t)} + (P - E) \cdot A_n(t) - \frac{Q_{out-\mathrm{n}}(t)}{R_c(t)} - \frac{W_n(t)}{R_c(t)} \quad (18)$$

where V_n is the total volume in the representative reservoir of class n (m^3), A_n is the representative reservoir free surface area for the n^{th} class (m^2), R_c is the reservoir count within the n^{th} class, and W_n is the withdrawal from the n^{th} reservoir class. Q_{out-n} is assumed to occur when storage capacity is exceeded. We assumed the latter approximation to be a good representation for the reservoirs of

smaller classes (1 through 4), as those classes represent the typical small earth dams seen in the region, where no outflow devices are installed. This assumption was also kept for medium-sized reservoirs, due to the absence of information on dam releases. Such an assumption was similarly followed in previous studies within the same region yielding satisfactory results (for example, Güntner et al., 2004 and Mamede et al., 2018). Finally, depth-volume-area relationships were used in conjunction with Equation 18:

$$V_n(t) = K_n \cdot h(t)^{\alpha_n} \tag{19}$$

$$A_n(t) = \alpha_n \cdot K_n \cdot h(t)^{(1-\alpha_n)} \tag{20}$$

where h represents water depth, while K_n and α_n are reservoir parameters taken as the average within each class n.

3.3.4. Water demand and its propagation throughout the reservoir network

The withdrawal term shown in Equation 18 is the result of the competition between the demand (D_n) and availability (V_n) for each reservoir class:

$$if: D_n(t) \leq V_n(t) \rightarrow W_n(t) = D_n(t) \tag{21}$$

$$else: W_n(t) = V_n(t),$$

$$and: DU_n(t) = D_n(t) - W_n\,(t)$$

where DU_n is the unmet demand (m^3), which is transferred to higher class reservoirs in a similar fashion as the outflows (Eq. 17). The demand applied to each reservoir is therefore composed of a local demand and a combination of unmet demands from smaller reservoir classes, whenever applicable:

$$D_n(t) = D_{n-local}(t) + \sum_{1}^{n-1} \frac{DU_{\mathrm{x}}(t) * f_r}{N - \mathrm{x}} \tag{22}$$

where $D_{n-local}$ (m^3) represents the demand imposed by the local population closer to a reservoir of class n. The variable f_r represents a reduction factor applied to the unmet demands from lower

reservoir classes when transferred to higher classes, resulting from the constraints involved in transferring water in contrast to the more promptly availability in nearby reservoirs. In this study, a value of 0.8 was adopted based on field survey with 502 families living within the Jaguaribe Basin, conducted in 2010 (Alexandre, 2012).

$D_{n-local}$ values were estimated through a combination of four different types of demand: rural (D_R), urban (D_U), large irrigation projects (D_{IP}), and industrial (D_I). D_R was estimated based on an average per capita demand (d_R), along with the population living in rural areas. d_R values were also obtained from the survey conducted by Alexandre (2012) and consisted of the sum between human-use, agriculture and livestock. Similarly, D_U was estimated based on a per capita demand of 120 liters per day (d_U) and converted to total volumes based on the population living in urban areas. The population totals, along with the rural and urban shares for the study area was obtained through censuses conducted by the Brazilian Institute of Geography and Statistics (IBGE) for the decades 1940 through 2020. For the 1920's and 1930's we assumed the value of 90% of the total UJ basin population to be living in rural areas. The irrigation projects are state-led projects for which specific reservoirs are designated. Thus, D_{IP} values were considered separately and were obtained based on the Water Resources Plan of the State of Ceará (Ceará, 2005), and were assigned to begin at the year of implementation of the perimeters. The industrial demand for the decades from 2000 to 2020 was obtained from the Secretary of Water Resources of the State of Ceará (SRH) and was taken to represent 1.8% of the State's total industrial demand (Ceará, 2005). For the 1990's, industrial demand was also obtained from the Water Resources Plan of the State of Ceará (Ceará, 2005), while no industrial demand was considered for the previous decades. Further detail on actual values (d_R, d_U, total volumes for D_{IP} and D_I) are shown in the supplementary material (**Table S2** and **Table S3**). Finally, the different demands were aggregated into values of $D_{n-local}$ according to the reservoir classes:

$$D_{1-local} = D_{2-local} = D_{3-local} = \frac{D_R}{3} \quad (21)$$

$$D_{4-local} = D_{5-local} = \frac{D_U}{3} + \frac{D_I}{3} \quad (22)$$

$$D_{6-local} = \frac{D_U}{3} + \frac{D_I}{3} + D_{IP} \quad (23)$$

4. Results

4.1. Dynamics of society and the reservoir system

The RSM properties, as implemented in the simulations in the IG basin are summarized in **Figure 3** and **Table**. The evolution of the population characteristics within the basin over the century shows an increase in the population living in rural areas from 1920 up to the 1970's, when it started to decline, while the share of urban population saw a constant rise since the 1930's up to recent years (**Figure 3a)**. As a result, it is possible to see in **Figure 3b** an analogous dynamic in demands for urban and rural water use. Figure 3 also shows the industrial demand, which started to compete for water in the 1990's. In this decade, the industrialization of the Ceará State commenced in the capital Fortaleza (located by the coast) but has expanded into the hinterlands since then. The growth of the total capacity of the reservoir system throughout the years can be depicted in **Figure 3c**, which shows a rapid increase from the 1950's following the intensification of the reservoir policy (Campos, 2015). Finally, a summary of annual streamflow data (mm per year) versus the total system capacity can be seen in **Figure 3d**, showing how, at the end of the simulation period, the system's total storage capacity has reached the mean annual streamflow for the IG basin. High storage capacity relative to runoff volumes has been documented throughout the entire Droughts Polygon: for instance, Medeiros and Sivapalan (2020) demonstrated that in the entire Jaguaribe Basin, where the UJ basin is located, this ratio reached nearly 2 after the implementation of the Castanhão, Orós and Banabuiú mega reservoirs.

The reservoir count and average properties per class used in RSM at IG basin are shown in **Table 1**, where it is possible to see that most reservoirs have low storage capacities: 85% of all reservoirs fall under class 1. However, class 1 reservoirs contribute only 5% to the total storage. This pattern is usual in other regions of the Droughts Polygon, where such small reservoirs are used mostly for cattle breeding and irrigation of small areas for livelihood (Alexandre, 2012). Finally, the distribution of the f fractions of HYMOD generated runoff in the different reservoir classes are shown in **Figure 4a**, where it is possible to notice no reservoir participation in the water balance until the 1950's decade, as highlighted in the figure inset. Also noteworthy is the relatively high contribution of runoff being directly routed to the catchment's outlet, as seen in the red line representing f_{out}. The curves representing the runoff influx into different reservoir classes show a pattern of increase in relative contributions with respect to the class's storage capacity, while the

growth pattern associated with each of them are the same as indicated by the overall growth progression shown in **Figure 3c.**

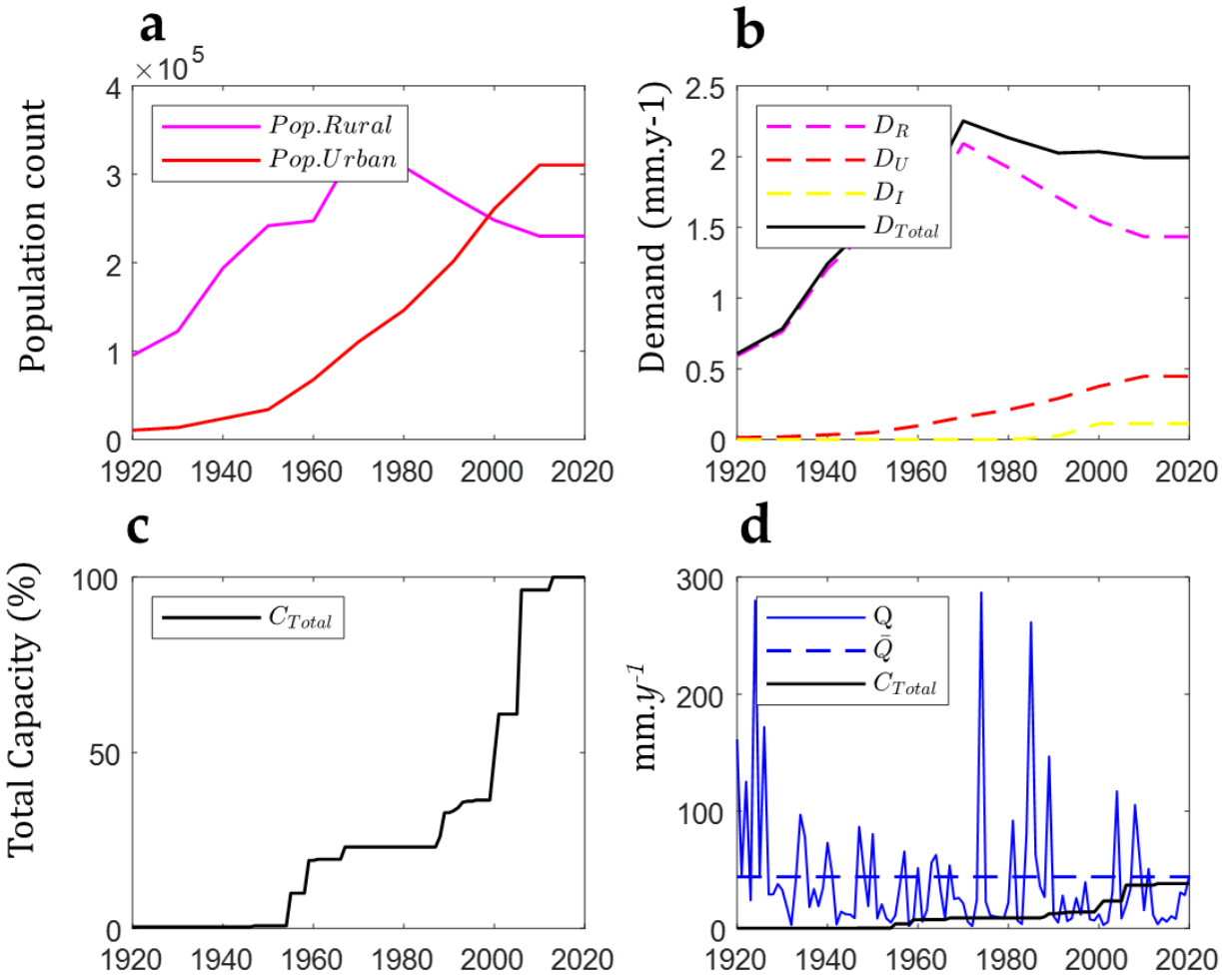

Figure 1. Temporal dynamics of society and the reservoir system in the Iguatu sub-basin. a - Distribution of urban and rural populations. b - Distribution of water demands (in mm/year). c - Evolution of the system's total storage capacity (in % of the total capacity). d - Comparison between annual streamflow values (solid blue line), mean annual streamflow (dashed blue line) (both in mm/year), and the total storage capacity (in mm).

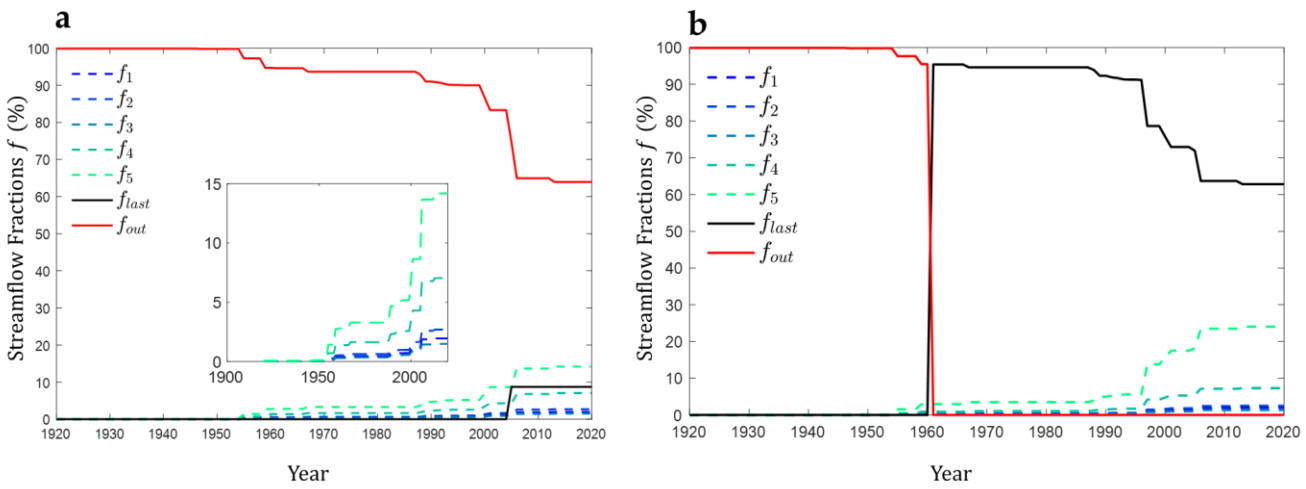

Figure 2. a - Distribution of the HYMOD generated streamflow as fractions between different reservoir classes and direct contribution to the outlet of the Iguatu sub-basin. b - Same as in subplot a, but for the Upper Jaguaribe Basin: A sudden change in the fraction of the runoff being directly routed to the basin's outlet (f_{out}) can be seen in 1960, the year of the construction of the Orós mega reservoir.

4.2. Model Performance

4.2.1. Calibration and Validation at the Iguatu Sub-basin

The effect of the introduction of the reservoir network scheme can be explored when comparing the model's ability to simulate streamflow at the IG basin's outlet. First, we explore the simulations using HYMOD only: while a good performance in terms of NSE was achieved for the monthly values of simulated streamflow during the undisturbed (calibration) period (**Table 2**), the same metrics have degraded during the validation period. When using the HYMOD combined with the RSM during the disturbed period, a better performance was achieved in terms of NSE between simulated versus observed streamflow, especially for the most recent decades, in which the reservoir network fully developed (**Table 2**). **Figure 5** shows a visual comparison of simulated and observed values of streamflow is shown for both HYMOD and HYMOD+RSM**,** where it is possible to see an overall reduction in streamflow at the outlet of the IG basin when the RSM is included. In terms of the slope of the regression line, the combined approach tends to reduce the magnitude of flows as seen by lower slope values when compared with HYMOD only results. This reduction is somewhat expected since the combined approach considers human withdrawals and evaporation from reservoir lakes.

Table 1. Comparison between NSE performance and slope of the observed vs. simulated of monthly streamflow at the Iguatu station using HYMOD only, versus HYMOD+RSM. Star (*) represents the 3 decades used for model calibration calibrated.

Period	HYMOD		HYMOD + RSM	
	NSE	slope	NSE	slope
1920-1930*	0.82	1.04	0.82	1.04
1930-1940*	0.72	1.10	0.72	1.10
1940-1950*	0.76	0.79	0.76	0.79
1950-1960	0.83	1.06	0.84	1.05
1960-1970	0.80	0.77	0.79	0.72
1970-1980	0.74	1.22	0.80	1.13
1980-1990	0.89	1.13	0.92	1.03
1990-2000	0.40	0.79	0.47	0.69
2000-2010	0.75	1.02	0.81	0.68
2010-2020	0.10	1.08	0.62	0.65

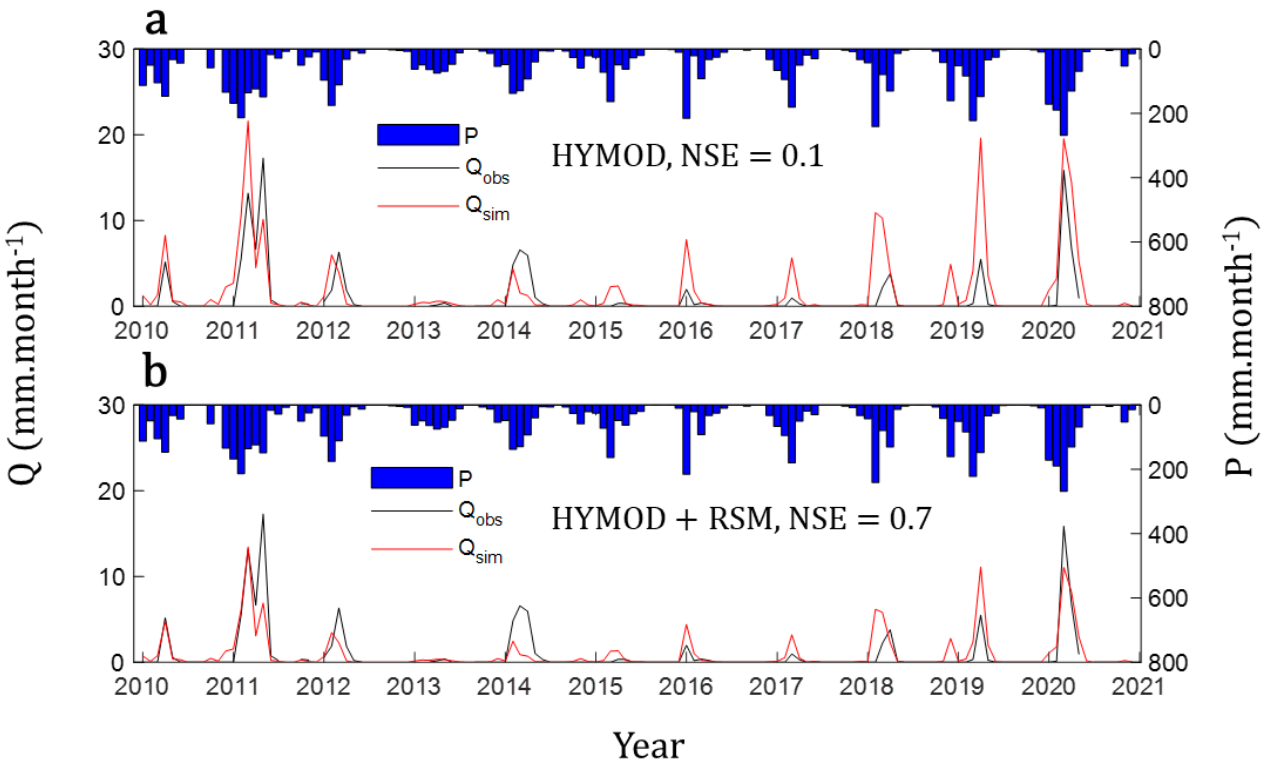

Figure 3. HYMOD model performance at undisturbed and disturbed period. a - Time series plot showing how monthly simulated streamflow values compare to observations using HYMOD only for the 2010-2020 decade within the disturbed period. b – Similar to subplot b but showing results for the HYMOD+RSM approach.

4.2.2. Validation at the Upper Jaguaribe Basin

To simulate water fluxes impacted by the dynamics of society and the reservoir network in a more representative basin of the Droughts Polygon, we applied the HYMOD-RSM model, calibrated to the IG sub-basin, to the whole UJ basin, which includes the mega reservoir Orós (1.94×10^9 m^3 storage capacity) in its outlet. The reservoir classification scheme implemented in the RSM at the UJ basin (**Table 1**) is very similar to what was previously utilized, with the main difference being the larger number of reservoirs per class and the existence of the Orós. For brevity, the growth in reservoir count for the UJ basin together with the distribution of demands throughout the years are shown in the supplementary material (**Figure S1**), since they are very similar to the ones at the IG station.

The distribution of the generated runoff of the UJ basin is shown in **Figure 4b**, which resembles the pattern for the fractional contributions f_1 through f_5. It is possible to see a switch between the fractional runoff being directly routed to the basin's outlet (f_{out}) and that being routed to the basins larger reservoir (f_{last}) in 1960, the year in which the Orós reservoir was built. f_{last} values tended to decrease over time as the basin experienced a growth in the number of smaller reservoirs, which therefore were responsible for capturing a fraction of the naturally generated runoff in the river basin.

Figure 6 shows a comparison between simulated versus observed values of volume being stored at the Orós reservoir. Our results suggest that the model has adequately captured the reservoir dynamics throughout the 1996-2020 period. Although measured volumes have been recorded since the mid-1980's at the location, no data on the reservoir release fluxes was available until mid-1990's, reducing therefore the length of the observed data. It is important to note that the model does not represent well the dynamics for the last three years of simulation. Given that calibrated model produced good results for the last 3 years of simulation in the Iguatu station (**Figure 5b**), we believe the discrepancies between observed and simulated volumes at Orós to be a drawback of our approach of applying the IG-based calibrated parameters for the whole UJ basin, in that runoff production, although satisfactorily represented for the calibrated portion, might not be adequate when including an additional area. We believe this result, as will be shown later on, will

not impact the main findings of our study, as our goal was to analyze larger temporal patterns of drought propagation, for which the last 3 years of simulation were not included.

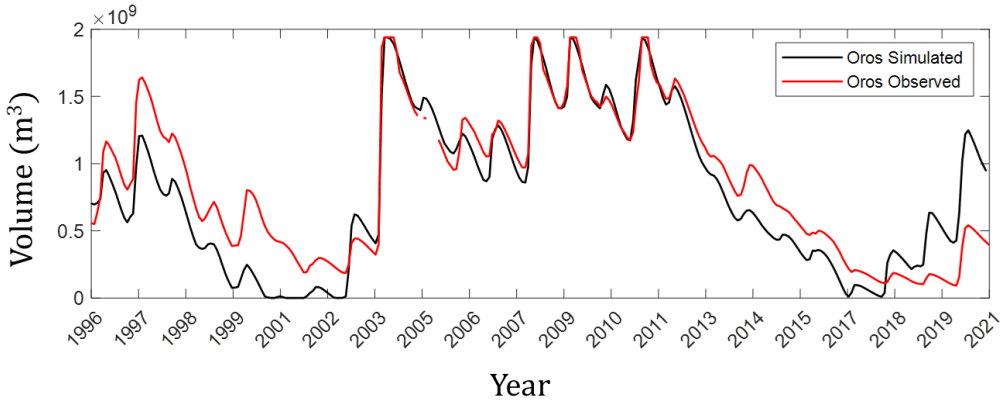

Figure 4. Model validation at the Orós reservoir, located at the Upper Jaguaribe outlet. Solid red and black lines represent the observed and simulated volumes, respectively.

4.3. Watershed Scale Impacts of Reservoir Network Expansion

The water balance dynamics over the 1920-2020 period is illustrated in **Figure 7**, indicating how the streamflow at the basin outlet changed following the reservoir network growth **(Figure 7a**). First, we can see the differences between streamflow values that contribute to the Orós reservoir: the streamflow entering the Orós reservoir (Qin altered, in red) shows consistently lower values than the naturally generated streamflow (Qin natural, in black), which is the streamflow that would have been generated at the same location if the basin had not experienced human-induced changes. This reduction in streamflow production was accompanied by an increase in evapotranspiration, as show in **Figure 7b,** where basin average values of annual evaporative fractions (E/P) are shown for two cases: the natural conditions (black line) as well as the actual systems conditions (red line). A slightly positive (not significant, $p=0.09$) trend in E/P values is shown to be associated with the natural conditions as shown in the black dashed line. When human intervention is considered, the positive trend is increased, becoming significant ($p<0.001$) as seen in the red dashed lines. Finally, in **Figure 7c** we show the impact of the reservoir expansion on streamflow permanence in the UJ basin. Here, we compare flow duration curves (FDC's) under natural conditions (solid black line) against FDC's produced by the combined effects of reservoir classes 1 through 5 (solid red line) as well as the full effect of the reservoir network, when the Orós dam is included (dashed red line).

It is possible to see the overall effect of reservoirs classes 1 through 5 as being responsible for a vertical shift in the FDC causing a reduction in the flow magnitude associated with all permanence percentages. On the other hand, the inclusion of the Orós dam results in increasing the flow beyond the 30% permanence while overall decreasing permanence below that threshold, when compared to the natural setting.

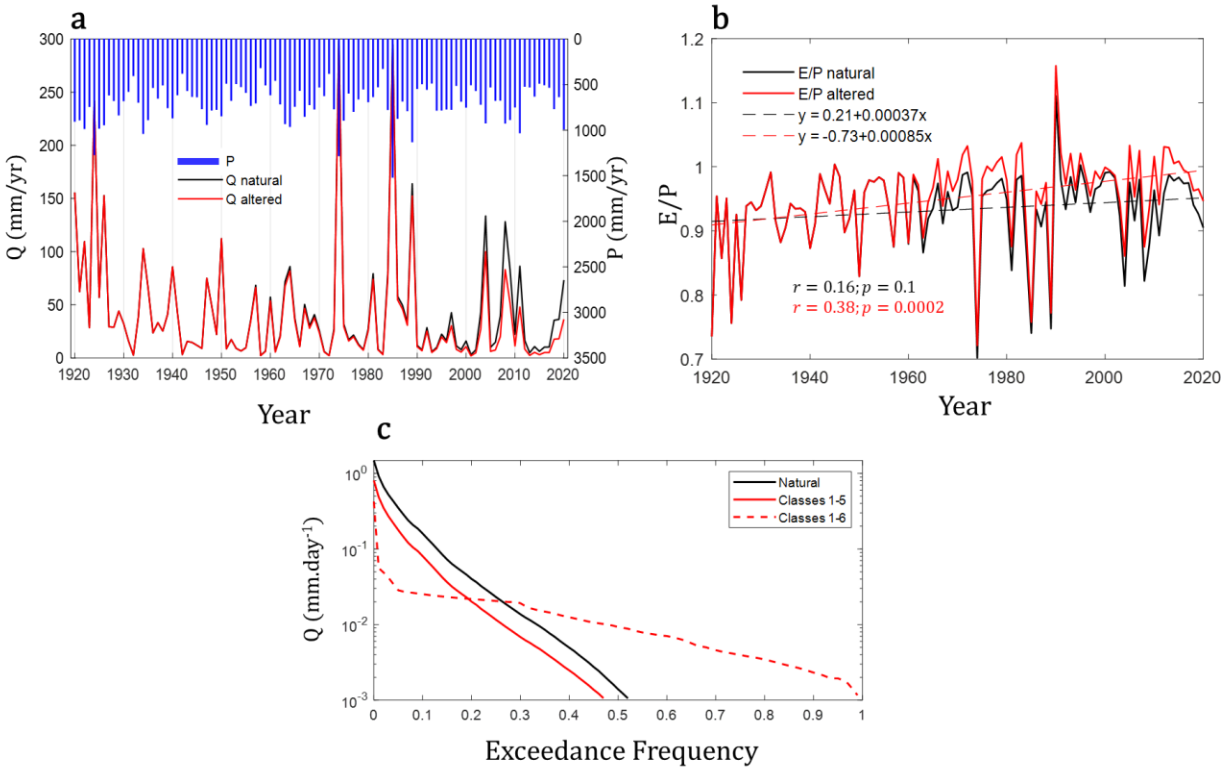

Figure 5. Impact of the dynamics of the reservoir system on the water fluxes at the Upper Jaguaribe Basin. a – Incoming streamflow at Orós reservoir at natural conditions (Q natural, in black), versus incoming streamflow when the reservoir network is considered (Q altered, in red). b – Annual E/P partitioning for natural (black) versus altered conditions (red), along with estimated linear trends. c – Flow Duration curve (FDC) at UJ basin considering the basins natural conditions (Natural, in black), versus FDC modified by the inclusion of reservoirs from classes 1-5 (Classes 1-5, in red), and FDC at the outlet of the UJ basin given the inclusion of all reservoirs (Classes 1-6, red dashed lines).

4.4. Decadal Patterns of Intra-annual Water Availability

To better characterize the evolution of the system, we aggregated the model results into monthly averages for 4 distinct decades, representing the periods before significant expansion of reservoir

network (1940-1950), during its initial expansion (1960-1970), intensification (1980-1990) and stabilization (2010-2020). We attempted to decouple the role of different drivers on the evolution of water availability and security as 3 distinct model simulations, shown in **Figure 8**: (i) the climate-only water simulation (C, in blue lines) represents water availability as the percent soil moisture (in percent of total soil storage capacity), and was chosen to depict the systems natural water availability, i.e., the water availability that would have been present without human interference. (ii) the climate and infrastructure (C+I, as black lines) simulation is based on a model run that considered only the infrastructure as it evolved over time, i.e., without withdrawal and represents the storage made available through the expansion of the reservoir network. In red lines, we show the actual (simulated) reservoir volumes for each reservoir class, considering withdrawal according to the prescribed demands (simulation C+I+H). Finally, for each decade and reservoir class, we computed an average water security index (α), as the average decadal values of percent demand met ($\alpha = \frac{demand\ met}{total\ demand}$), which is shown in each subplot.

The natural (soil moisture) availability within the system reflects the seasonal rainfall pattern at the UJ basin, leading to higher storage capacities in the months of March through May. Due to the lumped nature of the model, soil moisture estimates do not vary spatially (over distinct reservoir classes), and its temporal variability is associated with the decadal variability of rainfall. The effect of reservoir infrastructure (black lines) can be seen clearly as the extension of the water availability beyond the system's natural capacity: for each class, when comparing the blue and black lines, it is possible to see how water availability (in stored volume) extends beyond the humid months. However, it is important to note that for small reservoir classes (mainly classes 1 and 2), there are still months (on average) for which the system runs dry, which might imply significant portions of unmet demand, despite the existing infrastructure. With the increase in class number (and average storage capacity), this effect is less pronounced, with reservoirs not experiencing periods of very low to dry storage conditions. This simulated behavior, i.e., small reservoirs drying out frequently whereas larger reservoirs hold water for longer periods, is confirmed by field observations (see, for instance, Zhang et al., 2021).

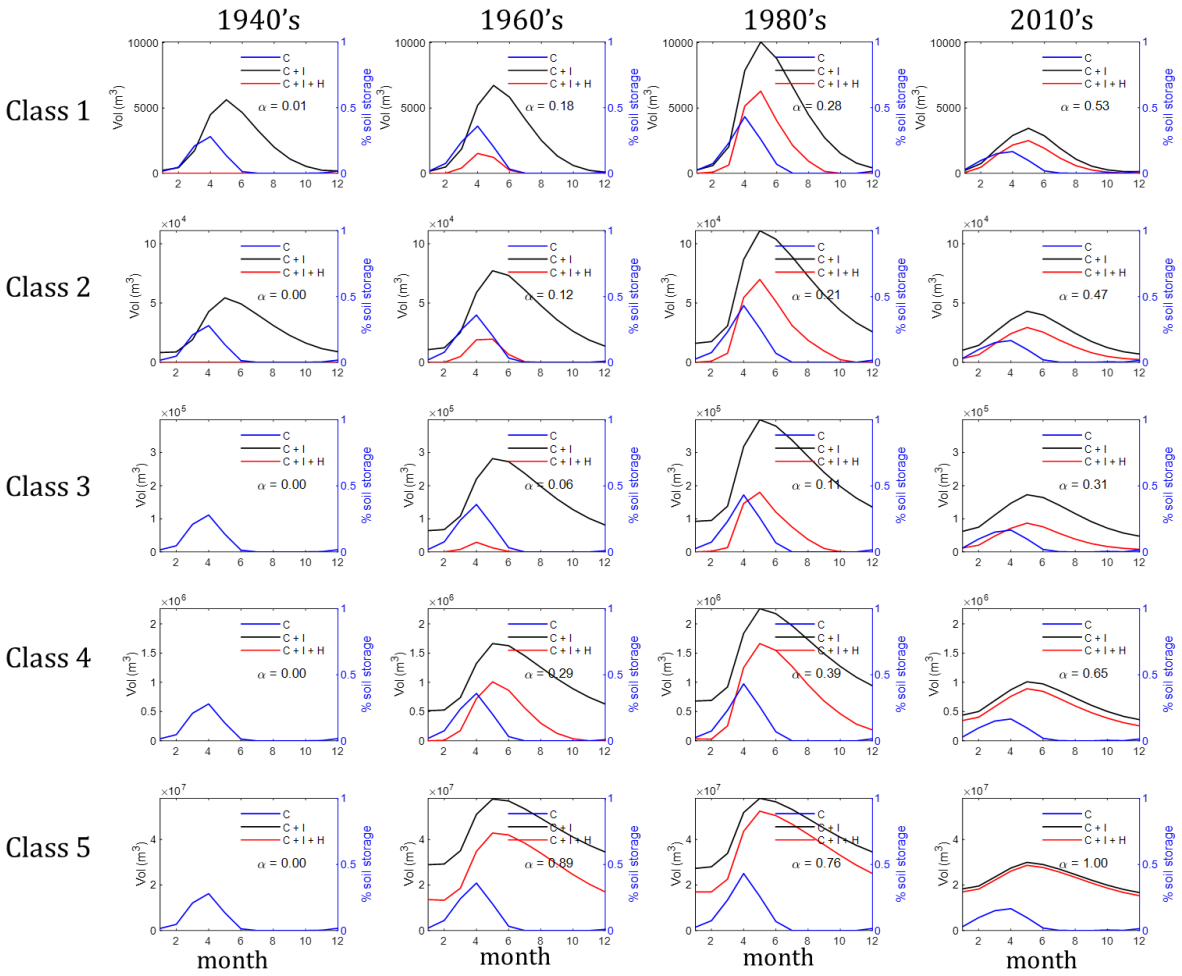

527

528 **Figure 8. Disentangling different drivers of intra-annual water availability and security through different**
529 **decades. Three simulations are shown at each subplot: in blue, values of average soil moisture throughout the**
530 **year, representing pristine water availability conditions, and is denoted as "C" (climate driven water**
531 **availability). "C+I" simulations (climate + Infrastructure), in black, show the reservoir-driven water**
532 **availability without withdrawals, to display the impact of the evolving infrastructure in the water availability.**
533 **Last, in red, "C+I+H" simulations (climate + infrastructure + humans)**

534

535 When human consumption is considered, an expected pattern is observed where the available
536 storage (black lines) is partially consumed, resulting in a vertical shift of the black lines towards
537 the red lines. With the systems' temporal evolution, this vertical shift decreases, due to the growth
538 in number of reservoirs, and an overall reduction of the population size relying on each individual
539 reservoir. This effect is captured as a widespread increase in α-values for all classes through the
540 decades. The observed decadal patterns clearly show an increase in water security driven by an
541 expansion of storage capacity. This can also be seen when considering watershed-scale α-values,
542 calculated per year (**Figure S2**), in which it is possible to see how the system was able to reach

543 average levels of water security around 90% at the beginning of this century. However, the increase
544 in water security over time is somewhat limited: α does not reach values closer to 1 in recent
545 decades for most reservoir classes, except for class 5 during the 2010-2020 decade. Thus, the
546 decadal averages of storage per reservoir class alone might not be sufficient to characterize the
547 dynamics of water security at the UJ basin. In the following section, we proceed with an inter-
548 annual assessment of the dynamics in water availability and security, to explore the factors shaping
549 the (somewhat constrained) observed growth in water security.

550 **4.5. Interannual Patterns of Water Availability During Drought Events**

551 To better understand the constraints in the resulting decadal evolution of water security, we
552 proceeded with an assessment of specific drought events. **Figure 9a and 9b** show the evolution of
553 the 2012 drought as seen through values of water security and reservoir storage according to
554 different simulation scenarios. This specific drought event was chosen to represent the drought
555 impact on water security for the given fully developed reservoir network. **Figure 9a** shows how α
556 varies throughout the years for reservoirs of different classes, along with the respective simulated
557 reservoir volumes. It is possible to see the effect of the drought in water security as α values and
558 reservoir volumes decrease from the year 2011 with the succession below average precipitation
559 values, followed by a recovery period around the end of the decade. It is also possible to see how
560 classes 4 and 5 are more resilient to droughts, since the decrease in α is lower for class 4, while
561 class 5 was able to maintain water supply at the full demand ($\alpha = 1$) for the same period.

562 Next, in **Figure 9b**, we attempt to explore the role of network expansion in explaining the observed
563 decrease in water security. For that, we show how the evolution of the 2010 drought through 2
564 additional C+I scenarios, where the system's storage capacity was fixed at prescribed stages:
565 namely at 15% of its current capacity (dashes and "x" symbols), associated with the year of 1987,
566 and 50% of its capacity (dashes and circles), as in 1990. Additionally, the reservoir volumes are
567 shown according to the current infrastructure, as solid black lines. These results show how the
568 same drought event would have propagated throughout the reservoir network given different
569 degrees of its expansion. The results show a clear impact of the network expansion in the severity
570 of drought events, as seen in the vertical shifts in water availability from lower levels of
571 development and higher storage values towards lower storage values associated with increasing

reservoir count. Not only that, but similar patterns can also be found for the duration of droughts, as seen in the time (as in number of years) elapsed from drought onset until initiation of recovery experienced within each class.

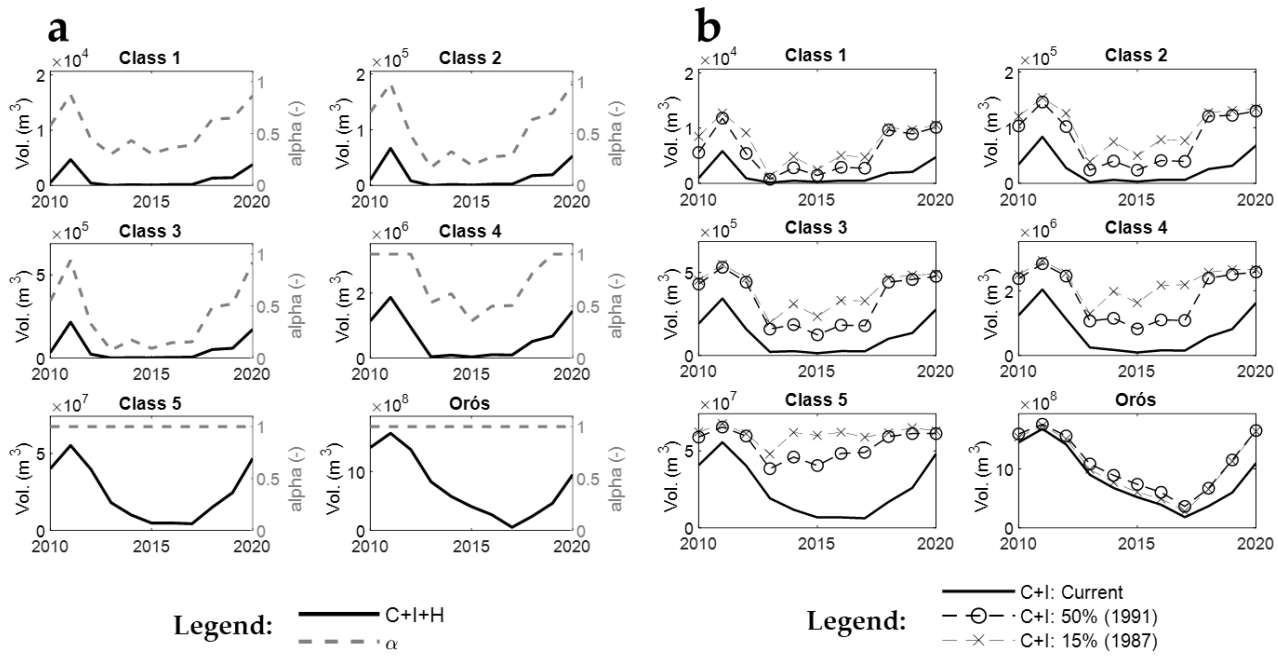

Figure 9. Impacts of reservoir expansion on the propagation of the 2010 drought at different reservoir classes and development scenarios. a-Progression of water security (α, in dashed lines) and storage values (solid lines). b-Scenario analysis comparing reservoir driven water availability (outputs from simulation C+I) at different development stages (as percent of the system's current storage capacity).

4.6. Role of Reservoir Expansion on the Evolution of Water Security and Drought Severity throughout the Decades

The analysis performed so far has shown that the observed decadal increase in water security associated with the reservoir network expansion was interrupted by the occurrence of drought events, which contributed to temporary increase of unmet demand during dry years. Additionally, when comparing the 2010 drought impact under different expansion scenarios (**Figure 9c**), we found the system's expansion to be associated with the increase in length and severity of that drought. We now seek to expand the insights gained so far to analyze whether such phenomena (system expansion and drought aggravation) can also be observed for different drought events

through different decades. We included 3 additional droughts occurring at different stages within the systems' expansion, namely the 1941, 1969 and the 1989 droughts (shown as red rectangles in **Figure 10a,** represented as sequences of below average precipitation anomalies).

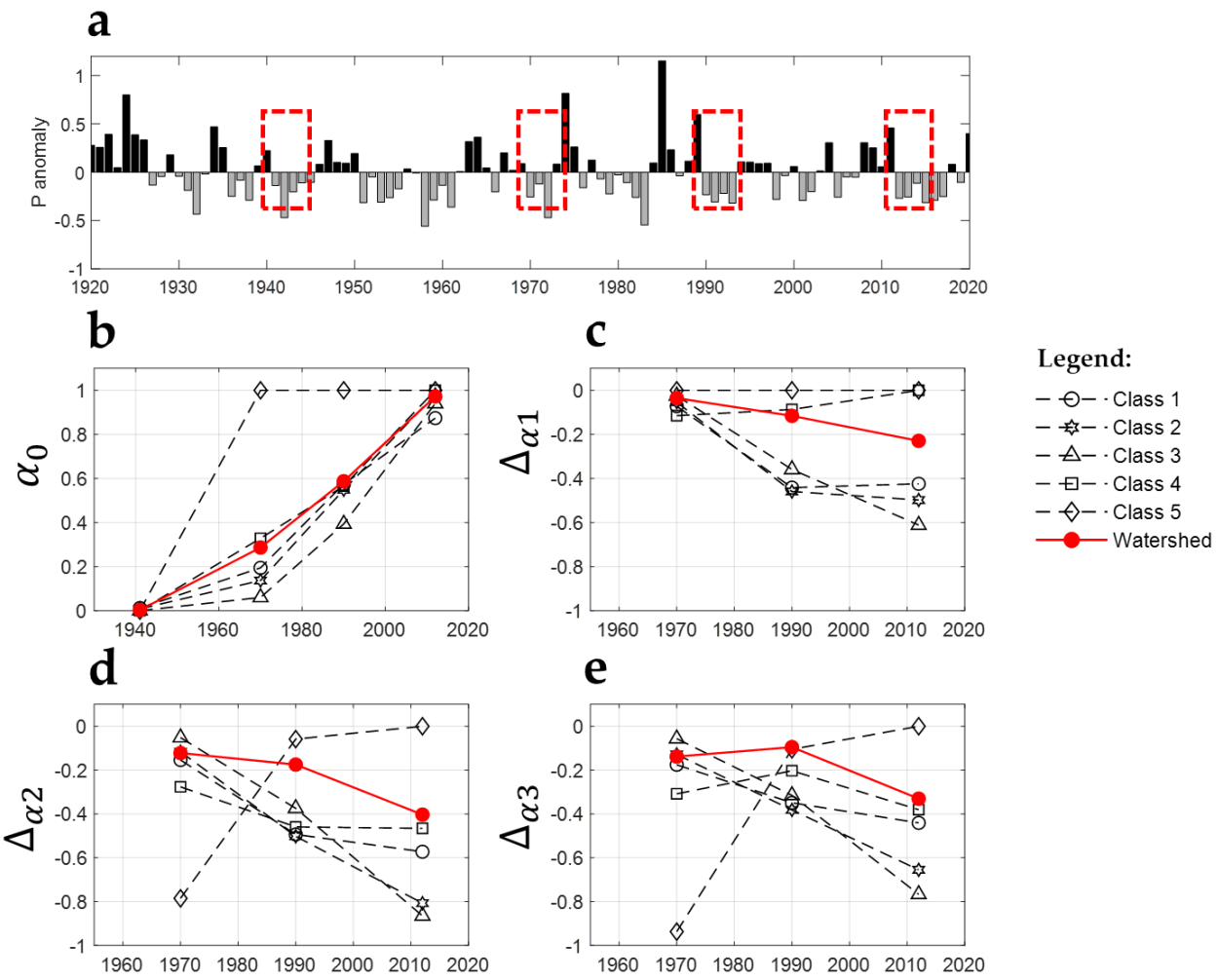

Figure 10. Temporal evolution of water security and drought impact. a: Interannual values of precipitation anomalies highlighting the chosen droughts. b: Pre-drought water security values, showing an increase in water

security prior to drought onset as a function of time. c through e: Drought impact (change in α from pre-drought values at years 1, 2 and 3 after drought onset, respectively).

In **Figure 10b**, we show the estimated water security values for each event for reservoir classes 1-5, and watershed-scale, at the year prior to the drought onset hereinafter referred as pre-drought water security estimates (α_0). Shown sequentially through **Figure 10c-e**, are the differences between α at subsequent years and those of α_0 ($\Delta\alpha_n = \alpha_0 - \alpha_n$, with n = 1, 2 or 3 years) as measures of drought impact for the years since drought onset. A clear pattern can be seen, in which water security values at the wet (pre-drought) years have increased over time (**Figure 10b**) at all reservoir classes, which is reflected in a similar trend in the watershed-scale α values. This phenomenon was accompanied, however, by different behaviors with respect to drought severity (**Figure 10c-e**): Watershed-scale negative trends (worsening of drought impacts) can be observed for the years after drought onset, which can be mainly attributed to reservoir of classes 1 through 4, while reservoirs of class 5 have experienced increasing resilience and capacity to accommodate such impacts. Reservoirs of class 4 have experienced a transitional response, showing a more stable response in the first year since drought onset (**Figure 10c)**, following a pattern similar to that of classes 1-3 in years 2 and 3 (**Figure 10d-e)**.

5. Discussion

5.1. Model Realism and Uncertainties

This paper presented a method for incorporating the continuous growth of a dense reservoir network within a hydrologic system over a 100-year period. Given the pressing need for modeling approaches that dynamically incorporate how humans interact with the water cycle (Srinivasan et al., 2017) over longer timescales, our study provides a simple, yet efficient, way forward to tackle the issue. Rather than the development of a purely predictive tool, our main goal was to provide broad insights into how the observed evolution of the reservoir network has affected the water balance at the UJ basin and to explore how the expansion of reservoir network has promoted human adaptation/settlement onto a once inhospitable region that had dealt through its history with the impacts of severe drought events. As such, the uncertainties in our modelling approach must be addressed.

Given the lack of data regarding actual historical growth in reservoir numbers for all classes, as well as their physical properties, the choice of a simple, yet conceptually sound, representation of the system and its growth was necessary, nonetheless allowing us to satisfactorily reproduce some important fluxes and stores observed in the basin. It is important to emphasize the complexity of the system in question (Peter et al., 2014): The dispersed nature of the reservoir system would make a distributed simulation practically infeasible. Explicit representation of reservoir networks has been attempted with the use of remote sensing techniques. For instance, Pekel et al. (2016) processed over three million images from the Landsat satellite to assess continental water occurrence at the global scale and its temporal dynamics. Within our study region, Zhang et al. (2021) retrieved the relief of reservoirs by using TanDEM-X data and mapped the storage variation of a network with high-resolution RapidEye images. However, remote sensing approaches fail to reproduce long-term changes in reservoir occurrence and water storage, since satellite images only became available from the 1980's. Therefore, such approaches alone are not able to capture the various temporal scales that drive the coupled human-water systems (Sivapalan and Blöschl, 2015).

Our model used, instead, an approximation to the prescribed human interventions, in that we have used historical data on populational growth and reservoir construction to drive the imposed changes in the hydrologic cycle. The approach presented here cannot be treated as a fully coupled socio-hydrologic model, as it does not consider some important two-way feedbacks operating over the decades in the UJ basin, as described by Medeiros and Sivapalan (2020). Understanding these processes would help us explain the observed growth in reservoir construction at the UJ basin, and why other feasible approaches that could have been taken by the local government did not happen.

5.2. Human Induced Changes in The Hydrologic Cycle.

The observation that the total storage capacity of the system reached approximately two times the mean annual runoff volume produced at the basin, points out the fact that the system has evolved from a condition in which water availability was limited by its low capacity to store water in the early 20th Century, i.e., a hydraulic constraint, to a hydrological limitation. Ultimately, this condition may lead to basin closure if the reservoir network continues to expand, a trend that has been observed in several large river basins around the globe such as the Colorado, the Indus, the

Murray-Darling and the Yellow (Molle et al., 2010). The shift in evaporation partitioning, driven by increasing water availability in the form of reservoir lakes, has been shown to be a detectable human imprint in the basin, and represents a drawback of the system. However, the evaporated volume of water may be affected by other features, such as: i) water use, as intensifying the withdrawals reduces the water level and the flooded area exposed to the atmosphere (Brasil and Medeiros, 2020); ii) riparian vegetation, which may reduce evaporation rates by up to 30% (Rodrigues et al., 2021). Despite its somewhat low magnitude, the statistically significant trends in the water balance partitioning found here represent an important result given the ubiquitous increase in evaporation, associated with the uncertainty in projected precipitation for the region in future climate scenarios, a combination which could potentially aggravate future water availability in the region (Rodrigues et al., 2023).

5.3. Emerging Outcomes of System's Evolution

The 100-year long reservoir expansion at the UJ basin promoted the region's transition from a state of extreme vulnerability to droughts and mass migration towards one characterized by stable human settlements and economic growth. This effect becomes clear when analyzing the population growth over the study period, along with other socio-economic indicators: population of the State of Ceará increased from 900 thousand inhabitants in 1900 to currently 9 million people, approximately, while improvement of the HDI were also observed, particularly from the 1990s, when it was 0.40 (very low human development) against 0.73 (high human development) in 2021.

The steady increase in water security throughout the decades observed in all reservoir classes was accompanied, however, by a heterogenous response in terms of the system's capacity to accommodate multiple drought events. System evolution led to a pattern in which large reservoirs were able to increase their capacity to attenuate drought impacts on water security (see the different responses between class 5 and other classes in **Figure 10**), while smaller reservoirs (Classes 1-3) experienced a diminished capacity to cope with such events. In spite of the recognized advances in water management in the study area since the 1990s, such an emerging pattern clearly denotes lack of centralized holistic water management strategy, which in the study region is due to the scarcity of data on small reservoirs and the limited operational capacity of the water resources management company. We argue that the reservoir expansion in the UJ basin arises as an

682 expression of the *aggregation effect* (Olson, 1965), a term coined to broadly describe how
683 individualized optimal decision making often leads to undesirable system scale outcomes.

684 How can we characterize the dynamics of the system in terms of the roles played by large versus
685 smaller reservoirs in water availability / distribution? Due to their limited storage capacity, smaller
686 reservoirs (Classes 1 through 3) are rarely sufficient to sustain the local demands for longer
687 periods, resulting in both direct and indirect effects observed in larger reservoir classes. These
688 classes are said to be hydrologically inefficient, and their *direct* effect can be observed as the
689 reduction in water available flowing into reservoirs of larger classes, with the *indirect* effect of
690 propagating the water demand throughout the reservoir network. On the other hand, larger
691 reservoir classes (Classes 4 and 5) are more likely to meet both local demands as well as the
692 "imported" (demand transferred from lower classes) over long periods of time and during
693 droughts. Such emerging outcomes caused by the observed hydraulic gradient are also associated
694 with a socioeconomic counterpart, as the population living in the basin headwaters and depending
695 on small reservoirs have the lower per-capita income in the region. As reservoir size increases in
696 lower regions, so does income associated with population depending on it: in the UJ, the largest
697 (100,000 inhabitants) and wealthier (USD 34,000 per capita GDP, as of Sept. 2023 currency
698 conversion rates) city of Iguatu is located immediately upstream of the Orós mega reservoir, at the
699 catchment outlet. For the entire Jaguaribe basin, the Castanhão mega reservoir (6.7×10^9 m³
700 storage capacity) located further downstream supplies water to the city of Fortaleza, whose per
701 capita GDP is USD 48,000 (value converted from local currency (R$) to USD according to Sept.
702 2023 conversion rates). Interestingly, this same hydraulic-and-wealth gradient can be seen as a
703 space-for-time analogue of the infrastructure development in the UJ Basin, where the populations
704 dependent on lower class reservoir are closer to early 1900's living conditions, being more
705 vulnerable to droughts than those downstream relying on larger storage capacities.

706 Whereas the large strategic reservoirs play a major role on providing water security, particularly
707 those of class 5 (see **Figure 10**), the smaller reservoirs contribute to its spatial distribution, also
708 contributing to energy efficiency by storing water closer to the consumers and at higher elevations.
709 Nascimento et al. (2019) assessed the impact of the reservoir density on the power demand for
710 water distribution in the Banabuiú basin (19,800 km²), also located in the Jaguaribe basin. The
711 authors concluded that, if the reservoirs with storage capacities below 5×10^5 m³ (which represents

712 the upper limit of class 2 in this study) did not exist, power demand would increase by 80%. If the
713 Banabuiú mega reservoir (1.4 x 10^9 m³ storage capacity) was the sole water source, the power
714 demand would increase by 30-fold.

715 It is worth emphasizing that the majority of smaller storage capacity reservoirs were built
716 spontaneously by the local population as a result of the political and economic constraints
717 experienced historically. We posit that such historical and socioeconomic mechanisms have played
718 a pivotal role in guaranteeing definitive settlement in a region that has experienced massive
719 migration due to historical droughts. In this context, the networks' *hydraulic* role has been to
720 provide the minimum conditions for such settlements to occur.

721 **5.4. Sociohydrologic Drivers of Reservoir Network Expansion.**

722 Could the reservoir system at the UJ basin have evolved in a different way? The understanding of
723 the diffuse nature of the system and its growth over time cannot be achieved without proper
724 acknowledgement of well-known historical socioeconomic drivers. The so-called "Dam Policy"
725 initiated in the early 20th century, when the first dams were built, and society experienced their
726 benefits. To expand the reservoir implementation, the Federal Government launched in the 1930s
727 the Cooperation Dam Policy, in which public funds were used to build dams on private properties
728 until the 1970s. Concomitantly, large strategic reservoirs were implemented by the Federal and
729 State governments to supply large demand centers, such as cities and irrigation projects. However,
730 access of rural population to the water sources remained limited, in a process named by Srinivasan
731 et al. (2012) as "resource capture by elite", encouraging the spontaneous construction of small
732 dams by the population. Such variability can be seen as an emergent property of the multiple socio-
733 political-economical processes that have taken place as the system evolved over time: the larger
734 reservoirs were built through public investment, whereas public-private partnerships were
735 involved in the construction of intermediate ones. Most importantly, community-led initiatives
736 resulted in the construction of small, short-lived reservoirs, that account for 95% of the dams built
737 in the region. Small-sized reservoirs appeared as a response from the local population to the
738 standing policy which favored large and medium sized reservoirs, most times located in private
739 (most likely access-controlled) properties.

More work is needed to unveil the socio-economic processes leading to the evolution of the system as has been portrayed here. Our approach can however be used to shed light and possibly aid investigations dealing with such questions, as it has been able to represent a long-known dynamic prevalent in Brazilian semi-arid system, especially within the state of Ceará (Campos, 2015), and its surrounding region. Further work focusing on the understanding of the history of sociopolitical and economic drivers of the observed system's evolution is in preparation and could lead to potential insights into the improvement of the model's parameterization. To achieve such a result, some conceptual improvements in our understanding of how humans have shaped the system's evolution might be necessary for future iterations of our model. For instance, the inclusion of drought memory as driver of water demand might allow for better characterization of drought impacts on human behavior (Song et al., 2020). Additionally, relationships between drought memory, and (suppressed) demand, paired with socio-economic constraints, might be leveraged to incorporate societal willingness to build dams, through both independent (local population) as well as through larger infrastructural investments.

6. Conclusions

The Drought Polygon, in the Northeastern portion of Brazil, occupies 12% of the country and has been historically plagued by droughts. Through the last century, the Upper Jaguaribe basin has experienced a transition from pristine conditions towards having a high-density surface reservoir network, possessing a great degree of variability in storage capacity (and technical complexity). This paper investigated the hydrology of the coupled human-water coevolution through the UJ Basin over the 1920-2020 period and attempts to shed light at the hydrologic outcomes of such expansion.

We introduced a parsimonious hydrologic model that enabled us to capture the dynamic evolution of storage capacity associated with reservoirs of various sizes, over a large, data-scarce region, where ca. 3000 reservoirs have been built. Human interference was incorporated by allowing the models structure to change, reflecting historical data on the reservoir construction, and by the use of a variable water demand, estimated through populational data. We used our model to track how water fluxes and security evolved over time and extracted patterns of its decadal and interannual

variability that can provide a diagnostic understanding of socio-hydrologic processes taking place through the reservoir expansion.

As expected, the UJ Basin experienced a steady increase in water security, allowing for the transition from complete vulnerability to drought events, towards a state in which values closer to 90% of the total populational demand is met on average. This increase in water security had arguably provided the necessary conditions for stable and secure human settlement in the area, together with promoting economic and populational growth. Such growth, however, resulted in increasing demands and spurred the expansion of the reservoir network even further, ultimately affecting the system's capacity to accommodate droughts, following a heterogeneous pattern: while populations relying on smaller reservoirs became more vulnerable over time, those relying on larger reservoirs have experienced increasing resilience to multiple year drought events.

Finally, this work represents the first step towards the development of a fully coupled socio-hydrological framework to explain how the reservoir expansion in the UJ Basin may have taken place. We envision further studies that will account for inclusion of the social and natural processes at the local scale and their associated feedbacks, such as the inclusion of restrictions to the access to water and the translation of water security and its variability into the population's memory as a driver of further reservoir construction.

OPEN RESEARCH

Data and Software Availability Statement

Analysis and generation of all figures from this work were produced using Matlab® 2022b. All compiled data used as inputs for the models developed in this work, together with Matlab codes used process those inputs, generate outputs and produce the figures are available through: https://doi.org/10.6084/m9.figshare.24251809.v2

ACKNOWLEDGEMENTS

CAPES: for the doctorate scholarship to Bruno Pereira and for funding the research stay of Pedro Medeiros at the University of Illinois at Urbana-Champaign, which originated this work (Finance code 001: Visiting Professorship Program 2017/2018, call nº 45/2017, grant 88881.173213/2018-01).

CNPq: for the research productivity fellowship granted to Pedro Medeiros and José Carlos de Araújo.

REFERENCES

Abeywardana, N.; Bebermeier, W.; Schütt, B. (2018), Ancient water management and governance in the Dry Zone of Sri Lanka until abandonment, and the influence of colonial politics during reclamation. *Water*, 10(12), 1746. https://doi.org/10.3390/w10121746

Aguiar, F. G. (1978), Estudos hidrométricos do nordeste brasileiro (Excertos). Boletim Técnico do Departamento Nacional de Obras Contra as Secas. Fortaleza, CE, 36 (2), 129–142.

Alexandre, D. M. B. (2012), Gestão de pequenos sistemas hídricos no semiárido nordestino. Doctoral thesis, Agricultural Engineering, Federal University of Ceará, Brazil. Available at: https://repositorio.ufc.br/bitstream/riufc/18913/1/2012_tese_dmbalexandre.pdf

Boyle, D. P., Gupta, H. V., & Sorooshian, V. (2000), Toward improved calibration of hydrologic models: Combining the strengths of manual and automatic methods. *Water Resources Research*, 36(12), 3663– 3674. https://doi.org/10.1029/2000WR900207

Bronstert, A., Araújo, J. C., Batalla, R., Costa, A. C., Francke, T., Förster, S., Güntner, A., Lopez-Tarazon, J. A., Mamede, G. L., Medeiros, P. H. A., Müller, E. N., & Vericat, D. (2014), Process-based modelling of erosion, sediment transport and reservoir siltation in mesoscale semi-arid catchments. *Journal of Soils and Sediments*, v. 14, p. 2001-2018.

Cai, X., Ringler, C., & You, J-Y. (2008), Substitution between water and other agricultural inputs: Implications for water conservation in a River Basin context. *Ecological Economics*, 66, 38-50. https://doi.org/10.1016/j.ecolecon.2008.02.010

Campos, J. N. B. (2015), Paradigms and public policies on drought in Northeast Brazil: a historical perspective. *Environmental Management*, 55(5), 1052-1063. https://doi.org/10.1007/s00267-015-0444-x

Ceará (2005), Plano Estadual de Recursos Hídricos (Water Resources Plan of the Ceará State: diagnosis). Fortaleza: Secretaria dos Recursos Hídricos – SRH. Available at: https://www.srh.ce.gov.br/planerh/

De Araújo, J. C., Bronstert, A. (2016), A method to assess hydrological drought in semiarid environments and its application to the Jaguaribe River basin, Brazil. *Water International*, v. 41, p. 213-230. https://doi.org/10.1080/02508060.2015.1113077

De Figueiredo, J. V., De Araújo, J. C., Medeiros, P. H. A., & Costa, A. C. (2016), Runoff initiation in a preserved semiarid Caatinga small watershed, Northeastern Brazil. *Hydrological Processes*, v. 30, p. 2390-2400. https://doi.org/10.1002/hyp.10801

Di Baldassarre, G., Wanders, N., AghaKouchak, A., Kuil, L., Rangecroft, S., Veldkamp, T. I. E., Garcia, M., van Oel, P.R.; Breinl, K., & Van Loon, A. F. (2018), Water shortages worsened by reservoir effects. *Nature Sustainability*, 1, 617-622. https://doi.org/10.1038/s41893-018-0159-0

Guerra, P. B. (1981). A civilização da seca. Fortaleza: DNOCS.

Heine, I.; Francke, T.; Rogaß, C.; Medeiros, P.H.A.; Bronstert, A.; Foerster, S. (2014) Monitoring seasonal changes in the water surface areas of reservoirs using terrasar-x time series data in semiarid northeastern Brazil. IEEE Journal of Selected Topics in Applied Earth Observations and Remote Sensing, 7, 3190-3199. http://dx.doi.org/10.1109/JSTARS.2014.2323819

Güntner, A., Krol, M. S., De Araújo. J. C., & Bronstert, A. (2004), Simple water balance modelling of surface reservoir systems in a large data-scarce semiarid region, *Hydrological Sciences Journal*, 49(5), -918, https://doi.org/10.1623/hysj.49.5.901.55139

Habets, F., Molénat, J., Carluer, N., Douez, O., & Leenhardt, D. (2018), The cumulative impacts of small reservoirs on hydrology: A review. *The Science of the Total Environment*, 643, 850–867. https://doi.org/10.1016/j.scitotenv.2018.06.188

Kuil, L., Carr,G., Viglione, A., Prskawetz, A., & Blöschl, G. (2016), Conceptualizing socio-hydrological drought processes: The case of the Maya collapse. *Water Resources Research*. v, 52 (8). 6222-6242. https://doi.org/10.1002/2015WR018298

Malveira, V. T. C., De Araújo, J. C., & Güntner, A. (2012), Hydrological impact of a high-density reservoir network in semiarid Northeastern Brazil. *Journal of Hydrologic Engineering*, 17(1), 109-117. https://doi.org/10.1061/(ASCE)HE.1943-5584.0000404

Mamede, G. L., Güntner, A., Medeiros, P. H. A., Araújo, J. C., & Bronstert, A. (2018), Modeling the effect of multiple reservoirs on water and sediment dynamics in a semiarid catchment in Brazil. *Journal of Hydrologic Engineering*, v. 23, p. 05018020. https://doi.org/10.1061/(ASCE)HE.1943-5584.0001701

Medeiros, P., & Sivapalan, M. (2020), From hard-path to soft-path solutions: slow–fast dynamics of human adaptation to droughts in a water scarce environment. *Hydrological Sciences Journal*, 65(11), 1803-1814. https://doi.org/10.1080/02626667.2020.1770258

Molle, F., Wester, P., & Hirsch, P. (2010), River basin closure: Processes, implications and responses. *Agricultural Water Management*, 97(4), 569-577. https://doi.org/10.1016/j.agwat.2009.01.004

Neves, F. C. (2007). A seca na história do Ceará. In S. Souza (Coord.), História do Ceará (4. ed.). Fortaleza: Fundação Demócrito Rocha.

Olson, M. (1965). The logic of collective action: Public goods and the theory of groups. Cambridge, MA: Harvard University Press.

Pekel, J. F., Cottam, A., Gorelick, N., & Belward, A. S. (2016), High-resolution mapping of global surface water and its long-term changes. *Nature*, 540, 418-422. https://doi.org/10.1038/nature20584

Pereira, B. S., Medeiros, P.H.A., Francke, T., Ramalho, G., Foerster, S., & De Araújo, J. C. (2019), Assessment of the geometry and volumes of small surface water reservoirs by remote sensing in a semi-arid region with high reservoir density. *Hydrological Sciences Journal*, 64,66-79. https://doi.org/10.1080/02626667.2019.1566727

Peter, S. J.; De Araújo, J. C.; Araújo, N. A.; Herrmann, H. J. (2014) Flood avalanches in a semiarid basin with a dense reservoir network. *Journal of Hydrology*, 512, 408-420. https://doi.org/10.1016/j.jhydrol.2014.03.001

Quan, Z., Teng, J., Sun, W., Cheng, T., & Zhang, J. (2015), Evaluation of the HYMOD model for rainfall-runoff simulation using the GLUE method. *Proc. IAHS*, 368, 180-185. https://doi.org/10.5194/piahs-368-180-2015

Ribeiro Neto, G. G., Melsen, L. A., Martins, E. S. P. R., Walker, D. W., & van Oel, P. R. (2022), Drought cycle analysis to evaluate the influence of a dense network of small reservoirs on drought evolution. *Water Resources Research*, 58(1). https://doi.org/10.1029/2021WR030799

Rodrigues, I.S.; Costa, C.A.G.; Raabe, A.; Medeiros, P.H.A. & de Araújo, J.C. (2021) Evaporation in Brazilian dryland reservoirs: Spatial variability and impact of riparian vegetation. Science of the Total Environment, 797, 149059. http://dx.doi.org/10.1016/j.scitotenv.2021.149059

Rodrigues, G.P., Brosinsky, A., Rodrigues, Í.S., Mamede, G.L., & de Araújo, J.C. (2023), Climate-change impact on reservoir evaporation and water availability in a tropical sub-humid region, north-eastern Brazil, Hydrology and Earth System Sciences Discussion. [preprint], https://doi.org/10.5194/hess-2023-189, in review, 2023.

Roy, T., Serrat-Capdevila, A., Gupta, H., & VALDES, J. A (2017), Platform for probabilistic multimodel and multiproduct streamflow forecasting. *Water Resources Research*, 53, https://doi.org/10.1002/2016WR019752.

Sivapalan, M., & Blöschl, G. (2015), Time scale interactions and the co-evolution of humans and water. *Water Resources Research*, 51 (9), 6988-7022. doi:10.1002/2015WR017896

Song, S., Wang, S., Fu, B., Dong, Y., Liu, Y., Chen, H. & Wang, Y. (2020), Improving representation of collective memory in socio-hydrological models and new insights into flood risk management. Journal of Flood Risk Management, e12679. https://doi.org/10.1111/jfr3.12679

Srinivasan, V., Lambin, E. F., Gorelick, S. M., Thompson, B. H., and Rozelle, S. (2012), The nature and causes of the global water crisis: Syndromes from a meta-analysis of coupled human-water studies, Water Resour. Res., 48, W10516, doi:10.1029/2011WR011087.

Srinivasan, V., Konar, M., & Sivapalan, M. (2017), A dynamic framework for water security. *Water Security*, 1, 12-20. https://doi.org/10.1016/j.wasec.2017.03.001

van der Zaag, P., & Gupta, J. (2008), Scale issues in the governance of water storage projects. *Water Resources Research*, 44(10), W10417. https://doi.org/10.1029/2007WR006364

van Langen, S. C. H., Costa, A. C., Ribeiro Neto, G. G., & van Oel, P. R. (2021), Effect of a reservoir network on drought propagation in a semiarid catchment in Brazil. *Hydrological Sciences Journal*, 66(10), 1567-1583. https://doi.org/10.1080/02626667.2021.1955891

van Oel, P. R., Krol, M. S., Hoekstra, A. Y., & de Araújo, J. C. (2008). The impact of upstream water abstractions on reservoir yield: the case of the Orós Reservoir in Brazil. *Hydrological Sciences Journal*, 53(4), 857-867.

Wang, D., Chen, Y., & Cai, X. (2009), State and parameter estimation of hydrologic models using the constrained ensemble Kalman filter. *Water Resources Research*, 45(11). https://doi.org/10.1029/2008WR007401

Zhang, S.; Foerster, S.; Medeiros, P.H.A.; de Araújo, J.C.; Montagh, M.; Waske, B. (2016) Bathymetric survey of water reservoirs in north-eastern Brazil based on TanDEM-X satellite data. Science of the Total Environment, 571, 575-593. https://doi.org/10.1016/j.scitotenv.2016.07.024

Zhang, S., Foerster, S., Medeiros, P., De Araújo, J. C., Duan, Z., Bronstert, A., & Waske, B. (2021), Mapping regional surface water volume variation in reservoirs in northeastern Brazil during 2009-2017 using high-resolution satellite images. *Science of the Total Environment*, v. 789, p. 147711, 2021.